Title
Tests of a Model Pole Assembly for the ALS U8.0 Undulator

Authors
Hassenzahl, W.V.
Phelan, D.

Publication Date
1992-04-01

LBL-31960
UC-406

Lawrence Berkeley Laboratory
UNIVERSITY OF CALIFORNIA

Accelerator & Fusion
Research Division

Tests of a Model Pole Assembly for the ALS U8.0 Undulator

W.V. Hassenzahl and D. Phelan

April 1992

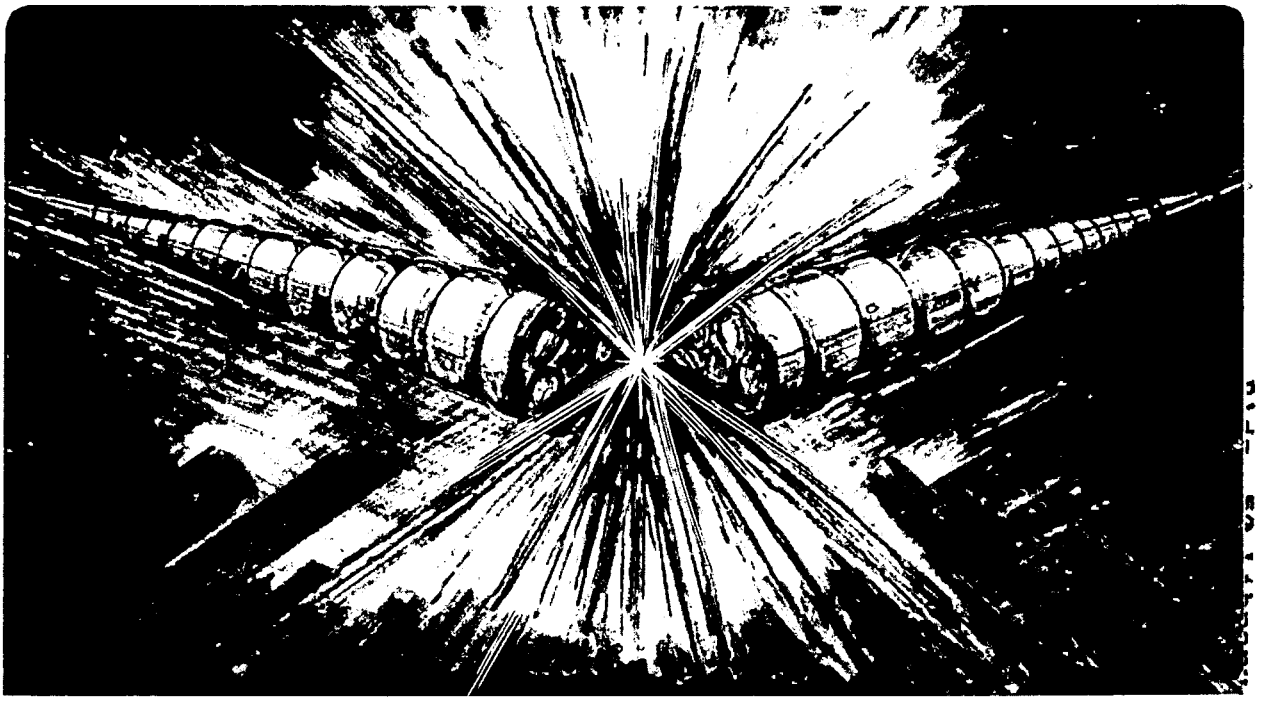

Prepared for the U.S. Department of Energy under Contract Number DE-AC03-76SF00098

This report has been reproduced directly from the
best available copy.

DISCLAIMER

LBL-31960

TESTS OF A MODEL POLE ASSEMBLY FOR THE ALS U8.0 UNDULATOR*

W. V. Hassenzahl, D. Phelan

Advanced Light Source
Accelerator and Fusion Research Division
Lawrence Berkeley Laboratory
University of California
Berkeley, CA 94720

April 1992

*This work was supported by the Director, Office of Energy Research, Office of Basic Energy Sciences, Materials Sciences Division of the U.S. Department of Energy, under Contract No. DE-AC03-76SF00098

Tests of a Model Pole Assembly for the ALS U8.0 Undulator

W. V. Hassenzahl and D. S. Phelan

ABSTRACT

The ALS insertion devices must meet very tight requirements in terms of field quality and field strength. Even though the ability to calculate the performance of a hybrid insertion device has improved considerably over the past few years, a model pole was assembled to test the ALS U8.0 undulator geometry and to verify the calculations. The model pole consists of a half period of the periodic structure of the insertion device with mirror plates at the midplane and at the zero-field, half-period planes. A Hall probe was used to measure the vertical component of the field near the midplane of the model as a function of gap and transverse position. Because of the tight field quality requirements, the ALS insertion devices are designed to permit several types of correction, including the capability of adding magnetic material or iron at several locations to boost or buck the field. This correction capability was evaluated during our tests. The model is described and details of the test results are discussed, including the fact that the measured peak field is higher than the calculated value, which is based on the measured magnetization of the blocks used in the model.

I Introduction

Insertion devices for the Lawrence Berkeley Laboratory (LBL) Advanced Light Source (ALS) and other third generation synchrotron light sources must meet more stringent tolerance requirements than insertion devices built to date for existing light sources[1]. Considerable effort has been dedicated to the development of requirements for the U8.0 undulator, which has an 8 cm period[2] and will be the second insertion device for the ALS. The design choice for high performance devices is a hybrid configuration with vanadium permendur poles and neodymium-iron-boron (Nd-Fe-B) permanent magnets. The performance of a device is determined by the peak field at minimum gap and the magnetic field errors. The importance of these characteristics is discussed in reference 2. The peak field as a function of gap can be calculated with a three dimensional theory of hybrid devices[3]. An extension of this theory[4] was used to estimate the field errors due to various material and assembly tolerances in the U8.0 insertion device. This paper addresses the peak field characteristics.

Calculations of the magnitude of the magnetic field in insertion devices have been found to be accurate to a few percent, which has been confirmed with calculations of the field for the beam line 10 (BLX) device at SSRL and for the TOK at NSLS by several approaches[5,6]. (Note that the peak field on axis of high performance devices is not a strong function of pole height. For example, increasing the U8.0 pole height from 6.2 to 9.6 cm while keeping other factors constant would

result in a field increase of only 7.4%.)[7] Even though this calculational capability exists, a half period model of the magnetic structure was constructed and tested to ensure peak field performance of the U8.0 undulator. This model pole assembly is a modified version of the U5.0 model pole shown in Fig. 1. The coordinate system used in this report is that typically used for insertion device analysis. The major field component, B_y, is measured here; the electrons pass through the device in the z direction, and oscillate in the x direction. The transverse field scans described in this report are in the x direction.

The U8.0 model was thoroughly tested to determine the peak field at the midplane and the transverse (x) variation of the vertical field. This data allowed an estimation of the effects of saturation in the vanadium permendur poles. The theoretical peak field calculated for the U8.0 blocks, which have a remnant field B_r of 11100 G, is 1.315 T. The measured peak field of 1.39 T drops to 1.369 T when adjusted for the models higher B_r and the hall probe's position above the midplane.

Because it may be necessary to tune the fields to meet accelerator or spectral requirements, one method of adjusting the magnetic field in ALS insertion devices was designed into the model. It consists of placing iron or permanent magnet inserts on the sides of the poles between the overhanging permanent magnet material. These inserts have two effects on the fields. First, they either boost or reduce the potential of the poles, and second, depending on the distance of the material from the midplane, they also cause a transverse redistribution of the midplane field.

This report describes in detail the model pole and the set of measurements made on it. It includes the following:

A description of the model pole.
A presentation of peak field at the midplane as a function of gap.
A discussion of the field variations due to various inserts.
A description of the transverse (x) variation in the vertical field due to side inserts.

II Description of the U8.0 Model Pole Assembly

The U5.0 model pole assembly is shown in Figs. 1 to 5. It was modified to produce a 5/8 scale model of the U8.0, consisting of: 1. a vanadium permendur pole; 2. two pairs of Nd-Fe-B blocks that are 0.85 cm thick, 5/16 the thickness of the U8.0 blocks; 3. a keeper that holds the pole and blocks in place and allows iron and permanent magnet material, sometimes called current (or charge) sheet equivalent material (CSEM) inserts or studs to be placed close to the pole; 4. a set of three mirror plates that define the magnetic symmetry of the device (one is at the midplane and one at each of the +/- 1/4 period planes); and 5. a mounting fixture, which simulates the backing beam. This fixture allows the pole to be positioned at distances above

the midplane corresponding to various gaps. Note that gap refers to measured half gap multiplied by 16/5 to provide equivalent U8.0 full gap dimensions.

The pole and the CSEM blocks model the upper (or lower) half of the U8.0 half period, the smallest unit of the periodic magnetic structure that can be modeled in this way. The blocks were made from left over Beamline 10 blocks that were cut and ground to the proper dimensions for this test. Each of these blocks are 1/2 the thickness, 3/2 the width (three blocks are modeled with two) and the correct height of a 5/8 scale U8.0 block. Because they were cut out of larger blocks in which the easy axis orientation was not completely uniform, they did not necessarily retain the magnetic moment orientation of the original BLX blocks, and may have larger transverse moments than the original blocks. Refer to Table I of U5.0 Model Pole Report[8] for magnetic characteristics of the blocks used for the U5.0 model pole.

The top piece of the mounting fixture is positioned a distance above the pole to simulate the position of the iron backing beam in the U8.0 geometry. Figure 2 shows the track at the bottom of the U5.0 model pole assembly that allows the Hall probe to be positioned under the pole. The probe can be moved in the x direction from one side of the assembly to the other. The position of the active component of the probe is about 1.0 mm above the midplane. This offset requires the measured fields B_m to be corrected to obtain the field B_0 at the midplane by using the relationship

$$B_0 = B_m [\cosh(2\pi\Delta y/\lambda_u)]^{-1} = 0.992\, B_m ,$$

where λ_u is the 5 cm (8 cm multiplied by 5/8 scale) period length.

The aluminum pole keeper shown in Fig. 3 has two tapped holes on each side that can hold iron or CSEM inserts. These inserts were all 5.6 mm (0.220") in diameter, 20.6 mm in length, and were held in threaded brass rods, which could be used to accurately position the inserts close to the vanadium permendur pole.

III The gap dependence of the magnetic field

The peak field was measured at several gaps. This field is the algebraic sum of all the spatial harmonics

$$B_p = \sum_{i=0}^{\infty} B_{2i+1}$$

The quantity of interest, however, is the effective field, B_{eff}, which enters into the calculation of the spectrum of the light emitted by the undulator. B_{eff} is given by

$$B_{eff} = \{ \sum_{i=0}^{\infty} [B_{2i+1}/(2i+1)]^2 \}^{1/2}$$

The relationship between the peak field and the effective field depends on the geometry of the device and can be found from the spatial field distribution, i.e., the magnitude of the spatial harmonics. The gap dependence of each spatial harmonic of the field is given by

$$B_{2i+1}(g1) = B_{2i+1}(g2)\exp(2\pi\{2i+1\}[g2-g1]/l_u).$$

The spatial field distribution can be calculated accurately by POISSON using the geometry and measured permeability of the pole as inputs. The theory of hybrid insertion devices developed by K. Halbach[4] can then be combined with these POISSON results to predict the peak field.

Precise ceramic gauge blocks (ground to a tolerance of 5μm) were used to set accurately the actual half gap of the model pole to 10.13 and 19.96 mm, corresponding to 3.242 and 6.387 cm gaps. These gauge blocks also prevented pole tilt. The half gap was adjusted to other values by using a precision depth gauge to measure the distance from the top of the mirror plates to the top of the backing beam. At each gap, the Hall probe scanned the transverse (x) direction while field and position were recorded.

The gap dependence of the measured peak field is given in Table I and in Figs. 6 and 7. The results of the field calculations, included in Table I, were produced by scaling the field according to the relationship $B = B_1 \cos kz + B_3 \cos 3kz$, where $B_3(1.4\ cm)/B_1(1.4\ cm) = 13\%$.

TABLE I
Measurements of peak fields

Gap (cm)	Measured Field (T)	Calculated Field (T)
1.4	1.3916	1.3855
2	1.0332	1.0411
3	0.6343	0.6704
4	0.4142	0.4426
5	0.2727	
6	0.1804	0.1988
7	0.1179	
8	0.0793	0.0903
9	0.0518	
10	0.0354	0.0411

The calculated fields are slightly smaller than the measured values at small gaps and about 10% larger at large gaps. The source of this discrepancy is not understood at this time. Fortunately, the measured fields are larger for small gaps. At a 1.4 cm gap the corrected measured peak field is 1.369 T, which yields an effective field of about 1.24 T. This field will allow for the production of photons with energies as low as 6 eV when the ALS is operating at 1.5 GeV. The original low energy photon requirement was 10 eV, corresponding to an effective field of about 1 T.

The magnitude of the peak field depends on the scalar potential (level of excitation) of the pole. The field distribution depends only on the geometry and level of saturation of the pole. Thus, for a given gap, the ratio of any spatial field harmonic to the fundamental will be independent of pole excitation (ignoring saturation and remanant field effects).

IV Magnetic Field variation in the transverse (x) direction

Transverse (x) profiles of B_y were obtained by moving the Hall probe, in 0.254 cm increments, from the field-free region on one side of the pole, x = 10.14 cm, to an equivalent position on the other side, x = -10.14 cm. The x positioning accuracy was about 0.0025 cm, using a Compumotor/Daedal stage system controlled by a PC. The output of the Bell Gaussmeter was measured with a digital voltmeter and read into the PC using an IEEE-488 interface.

Figure 8, a transverse scan for the 1.4 cm gap, shows that the field under the pole is relatively flat from -1 cm to +1 cm. The magnetic field decreases as the edge of the pole is approached. At the edge of the pole (2.5 cm from the pole center) the field has dropped to about 70% of the central value. The magnetic field approaches zero at 8 cm from the pole center.

Field measurement repeatability is quite good, although the pole moved in the keeper structure slightly when inserts were installed. Figure 9 shows the difference between two measurements of presumably identical fields. In the central two centimeters the repeatability is about 0.01% of the central field, with the maximum field difference of 0.08% occuring in the region of strong field gradient at the edge of the pole. This is presumably due to the positioning error. The field gradient (change in field divided by change in position) multiplied by an estimated 0.0025 cm positioning accuracy is also shown in Figure 9.

The field distribution near the center of the device affects the spectral performance of the insertion devices and the operation of the storage ring. Figures 10 and 11 show the normalized magnetic field near the center of the device for gaps of 1.4, 3.242, 6.387 and 13.17 cm.

Figure 12 shows the differences between the normalized (subscript n) field values for different gaps ($B_{yn}(1.4)$-$B_{yn}(3.24)$, $B_{yn}(1.4)$-$B_{yn}(6.387)$, $B_{yn}(1.4)$-$B_{yn}(13.17)$) as a function of transverse (x) position. The graph shows that, as expected, small gaps have a strong gradient near the edge of the pole, whereas larger gaps have a weaker gradient over a wider distance.

V Field modifications due to "shims"

A major concern in the design of an insertion device is that the magnitude and/or distribution of the error fields exceeds the specifications. The underlying philosophy in ALS insertion device design is to limit errors by assigning tight tolerances. But, as a fallback position, the ALS insertion device design includes several methods of local field correction. The U5.0 and U8.0 model pole assemblies were used to evaluate two methods of adjusting the field; either CSEM or iron inserts were placed on the sides of the pole. The CSEM inserts were magnetized along the length (or axis) of the cylinder, boosting the central magnetic field (and the potential of the pole). The iron inserts affected the capacitance of the pole and led to a reduction in central field. Because of the model geometry, i.e. there are mirror planes at the quarter period points, the effect of any pole modification is the same as if all poles had received the same relative change in scalar potential. It is the same as adding inserts to each pole in the periodic structure. The U5.0 model pole report contains a more detailed analysis of the effects of inserts.

Field measurements with inserts in place were analyzed as field difference maps developed via the following procedure. First, a gap was set and a transverse scan was recorded without inserts to establish a baseline. Second, several scans with various insert configurations were recorded. Third, all inserts were removed and another baseline scan was made. The first and the last baseline scan were compared for changes and to determine repeatability. The difference maps were obtained by subtracting the average of the baseline scans from the field with inserts. These curves were then normalized to the peak field in the baseline runs.

VI Effect of CSEM inserts on the lateral field distribution

Two typical difference maps, with one and two CSEM inserts in the bottom position, are shown in Fig. 13. The pair of inserts boosted the field under the pole by about 0.35%. The large field excursions at about ±7.2 cm are caused by flux that goes directly from the "magnetic charge" at the end of the insert to the midplane, which is a graphic example of the direct field[4]. The field in the center of the device is boosted twice as much for two inserts as it is for one; within the accuracy of the measurements the inserts obey the superposition law. This suggests that saturation does not degrade the effect of the inserts.

A drawback of most correction schemes is that they are gap dependent, making it possible to shim the device at one specific gap perfectly, but often by reducing the performance of the device at other gaps. Except for small gaps, the field produced by the inserts tracks that produced by the main CSEM (Fig. 14). Our suspicion is that these differences are caused by saturation effects in the pole. There is a significant variation in the normalized change of the central field and the field difference from a 1.4 cm gap to a 3.0 cm gap. Even though the model does not simulate the effect of a change in only one pole, it gives a good indication of the usefulness of this approach for error control. This suggests that a correction valid at 1.4 cm would be about twice as strong as necessary at gaps of 3.0 cm and greater.

VII Effect of iron inserts on the lateral field distribution

The effect of iron inserts on the transverse field distribution was also studied. Figure 15 shows the results of a scan with iron in the bottom right position, and a scan with the iron in the top right position. For the bottom position, the large peak at 7 cm is caused by the direct fields of the insert. The field change under the pole is not constant but shows a gradient. The gradient suggests that there is a vector potential drop along the pole, which is a sign of pole saturation. The field change under the pole for the insert in the top position is nearly independent of the insert height. Note that there are practically no direct fields in the midplane for the insert in the top position as evidenced in the lack of peaks beyond the edge of the poles.

VIII References:

1. A. M. Fauchet, B. C. Craft, J. N. Galayda, H. Hsieh, A. Luccio, J. B. Murphy, C. Pellegrini, A. van Steenbergen, G.Vignola, L. H. Yu, R. R. Freeman, and B. M. Kincaid, "Beamline U13-TOK", Brookhaven National Laboratory Annual Reports 1985 and 1986.

2. ALS Insertion Device Design Group, "U8.0 Undulator Conceptual Design Report", PUB-5276, (May 1990).

3. K. Halbach, "Design of Magnets", Jülich videotape lecture series, (May to June, 1985).

4. K. Halbach, "Design of hybrid insertion devices", LBL lecture series, (October, 1988 to March 1989).

5. B. M. Kincaid, "Analysis of Field Errors in Existing Undulators" NIM Vol. A291, Nos. 1,2, (May 20, 1990).

6. Private communication, D Humphries, Lawrence Berkeley Laboratory.

7. R. Savoy, W.V. Hassenzahl, "Periodic Magnetic Structure Design Calculations for U8.0", LSBL - 131, LBL Report LBL - 32025, (June 1992).

8. W.V. Hassenzahl, E. Hoyer, R. Savoy, "Tests of a Model Pole for the ALS U5.0 Undulator", Published in the Proceedings of the 1991 Particle Accelerator Conference, May 1991, IEEE Conference Record, 91 CH 30 38-7, pp. 2736–2738..

Figure Captions

Fig. 1. Photograph of the U5.0 Model Pole.

Fig. 2. Cutaway view of the U5.0 Model Pole showing the various components.

Fig. 3. Photograph of the pole keeper for the U5.0 Model Pole

Fig. 4. Details of the of the CSEM and Vanadium permendur for the U5.0 Model Pole.

Fig. 5. Detail of the cutaway view showing the pole, magnetic blocks, Hall probe, and the alignment features.

Fig. 6. A comparison of measured and calculated peak fields for the U8.0 model as a function of gap.

Fig. 7. Measured gap dependence of the peak field on a logarithmic scale.

Fig. 8. Transverse (x) field distribution for 1.4 cm gap, maximum field is 1.392 T.

Fig. 9. Difference of two scans at 1.4 cm gap showing repeatability of the field scan, and gradient multiplied by positioning accuracy.

Fig. 10. Normalized field variation as a function of transverse (x) position.

Fig. 11 Normalized field variation as a function of transverse (x) position.

Fig. 12 Plot of the difference in the normalized fields for various gaps.

Fig.13 Change in the field due to CSEM inserts for a 6.387 cm gap .

Fig. 14 Unenergized and energized field differences (field with inserts less field without inserts at x=0) for various gaps.

Fig. 15 Transverse (x) variation in field for a 1.4 cm gap due to an iron insert in the each position on right side.

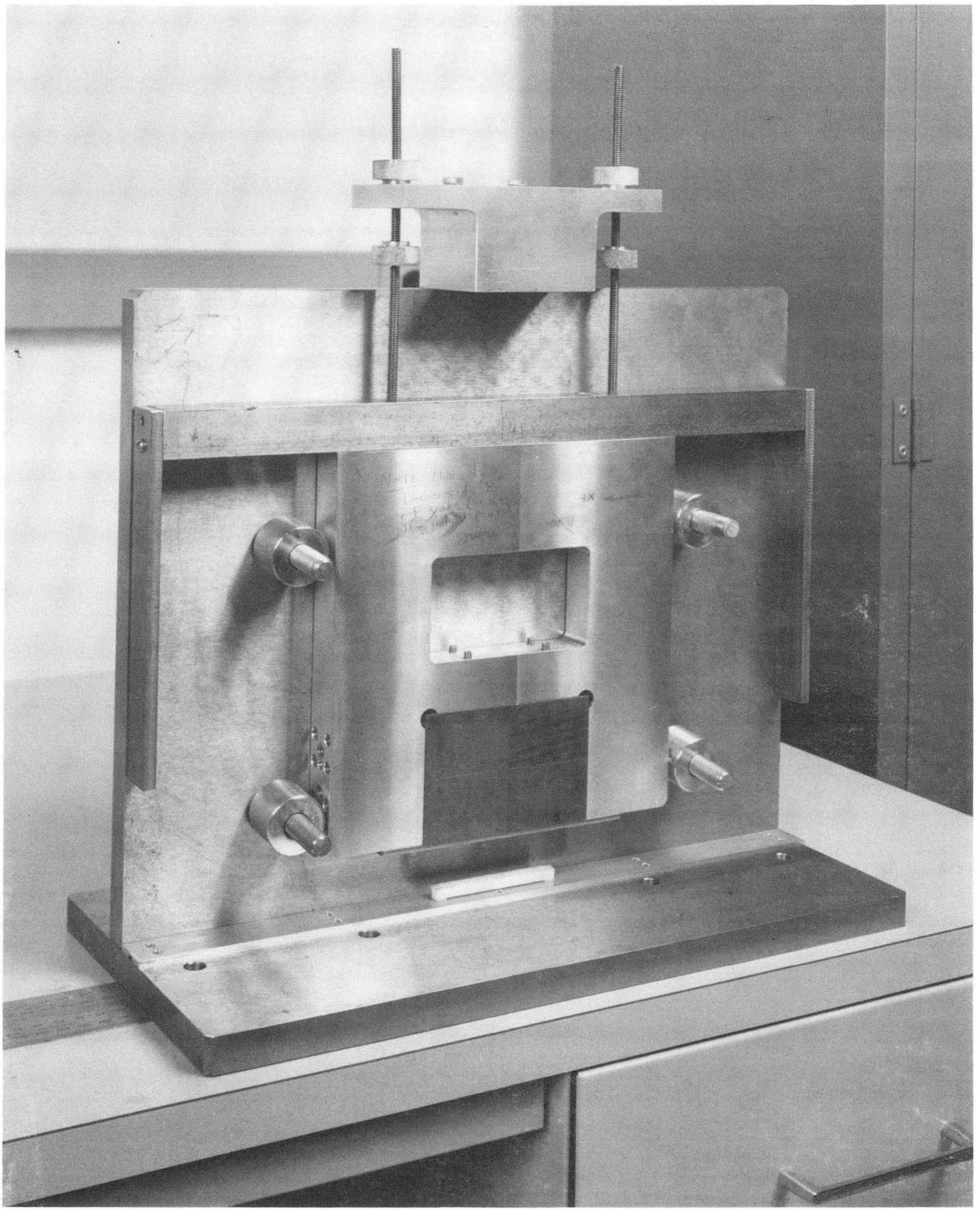

CBB 901-409

Fig. 1

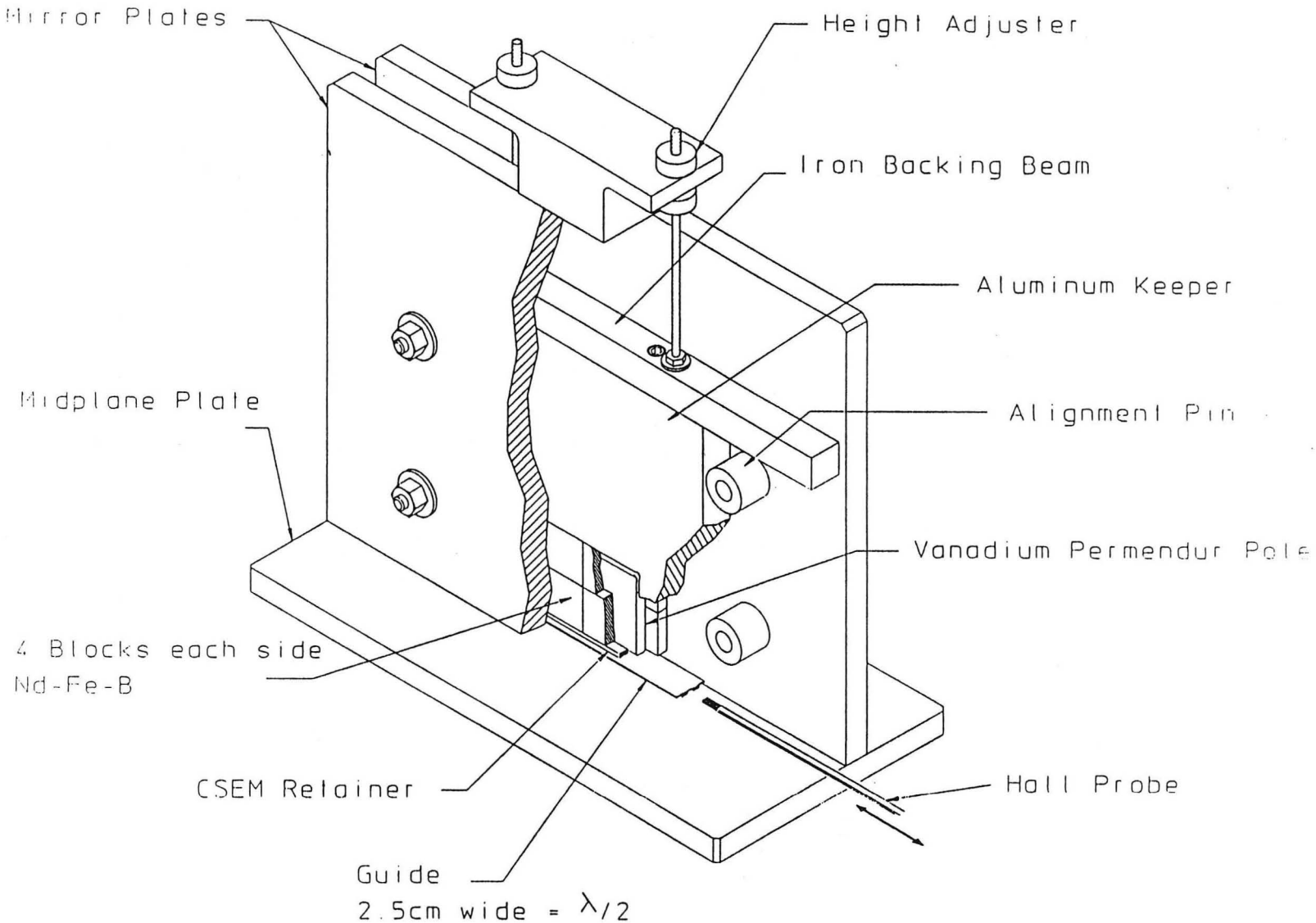

Fig. 2. Cutaway view of the U5.9 Model Pole showing the various components.

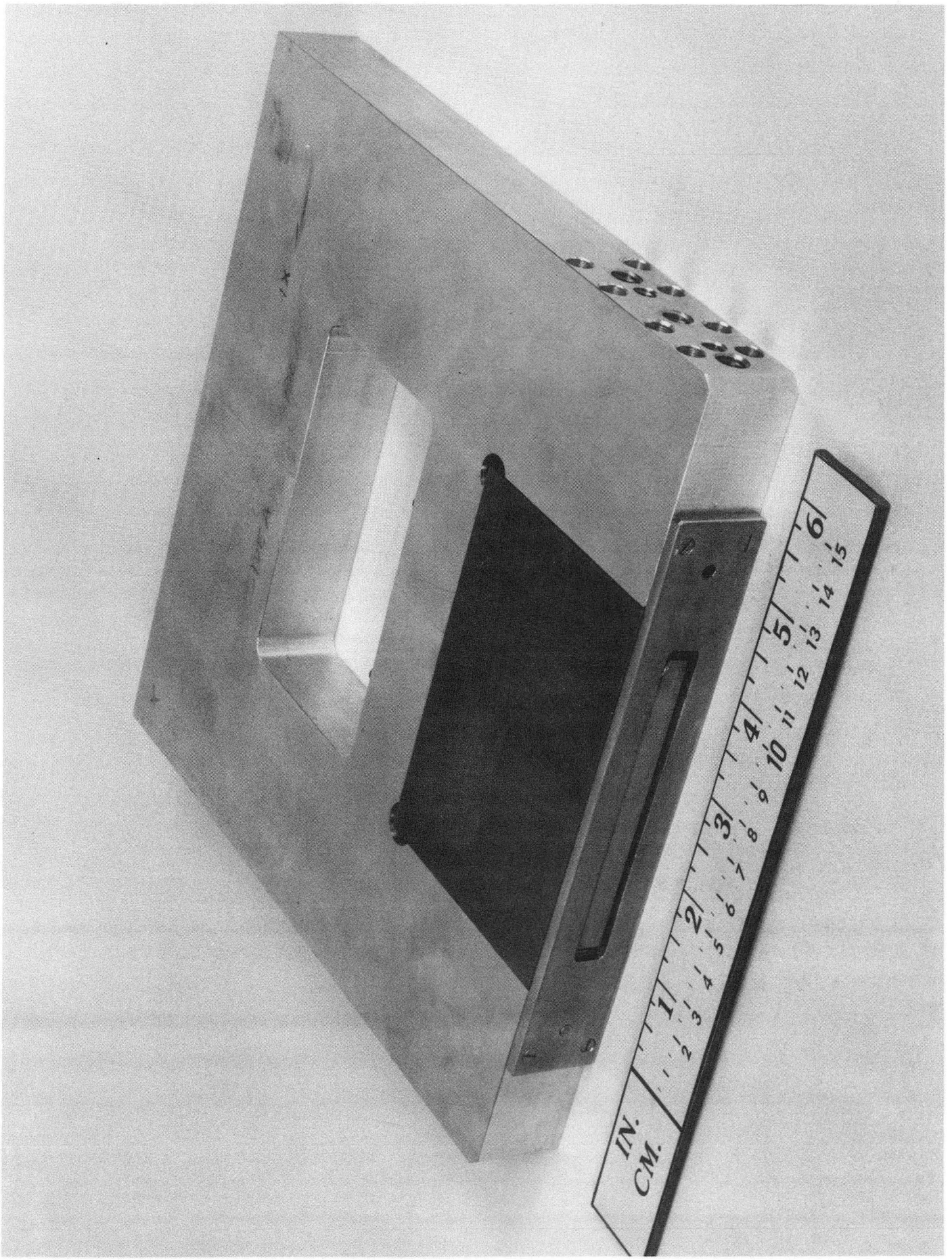

Fig. 3.

CBB 901-312

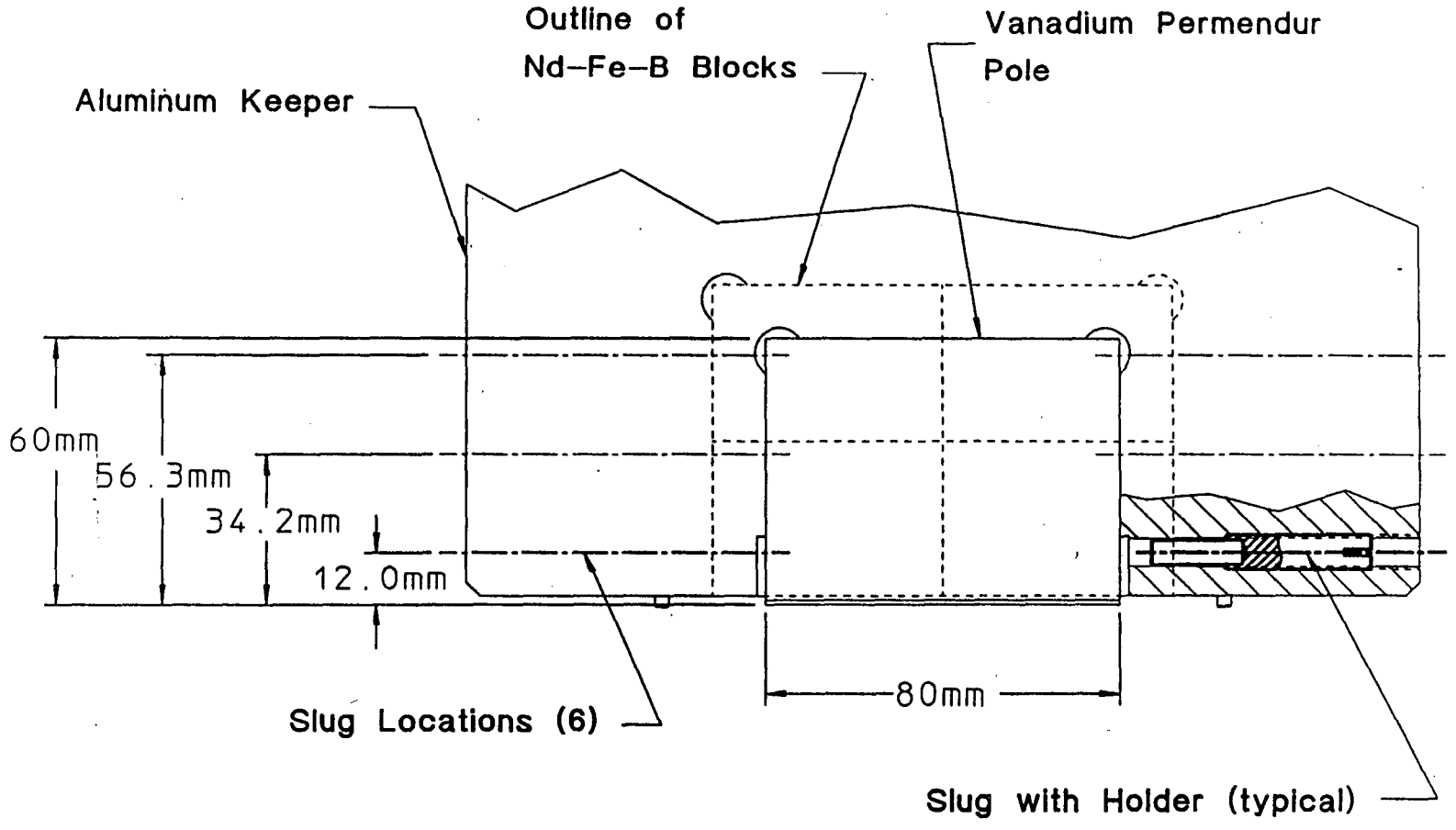

Fig. 4. Details of the of the CSEM and Vanadium permendur for the U5.0 Model Pole.

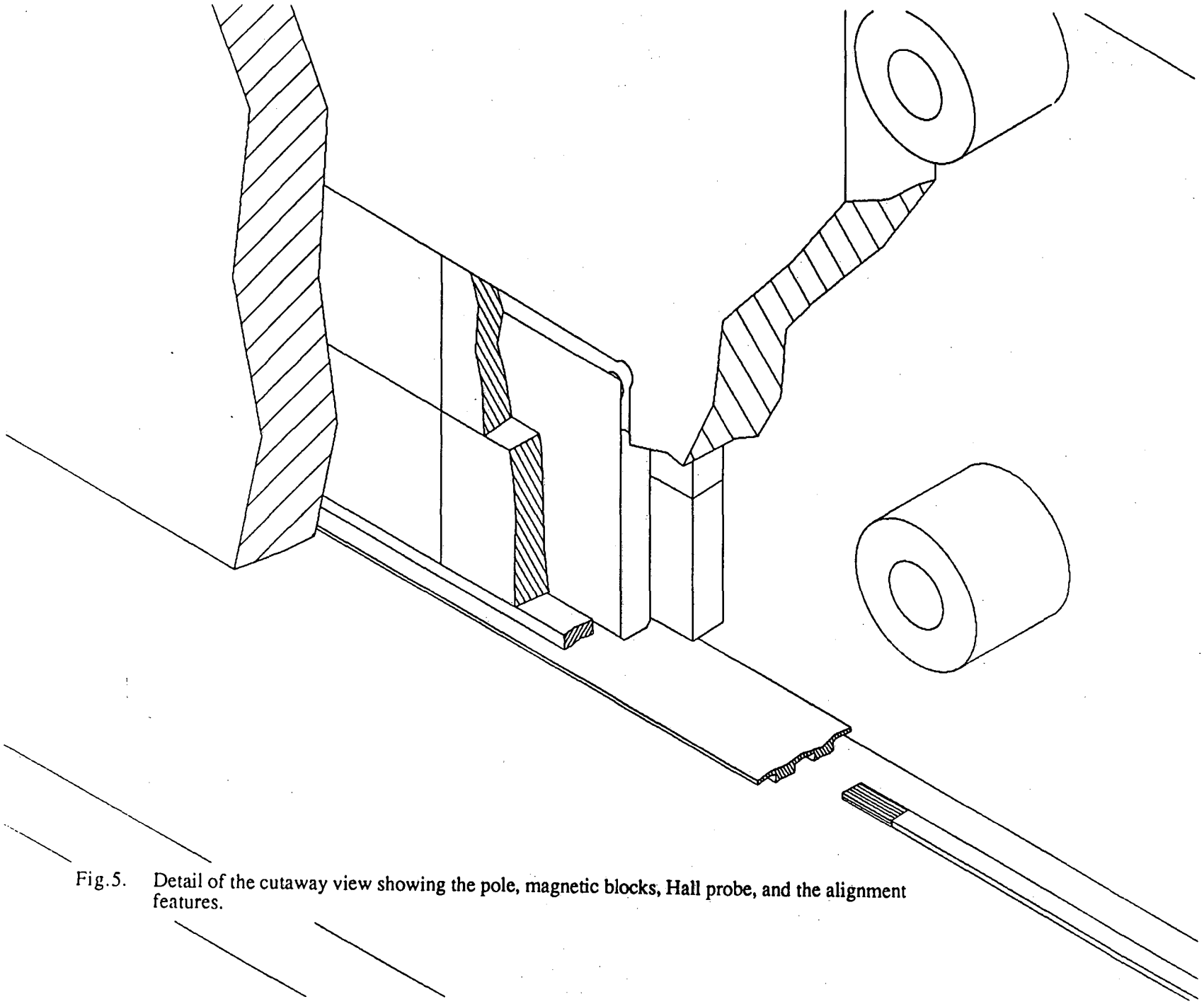

Fig.5. Detail of the cutaway view showing the pole, magnetic blocks, Hall probe, and the alignment features.

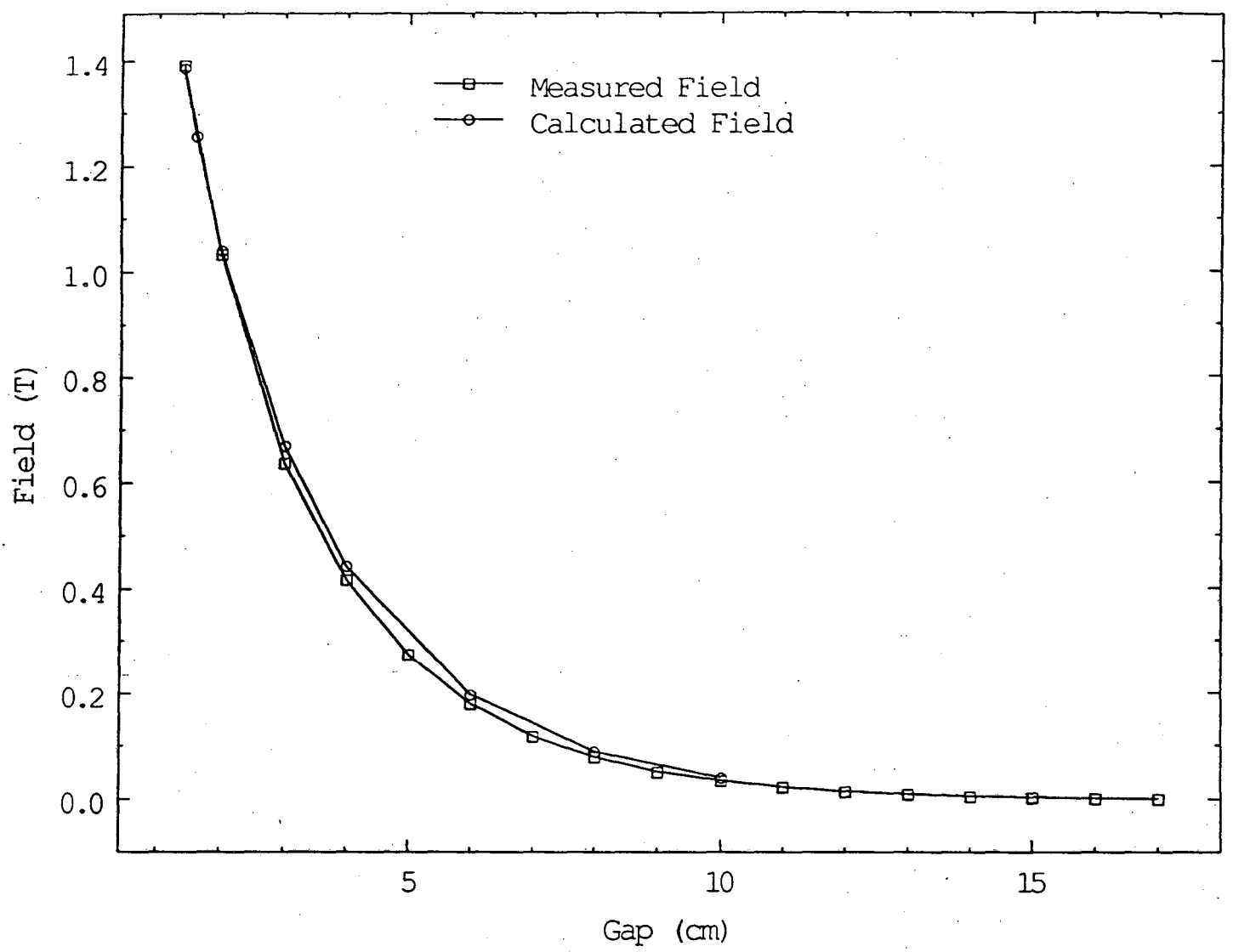
Measured Field
Calculated Field
Field (T)
1.4
1.2
1.0
0.8
0.6
0.4
0.2
0.0
5
10
15
Gap (cm)

Fig. 6.

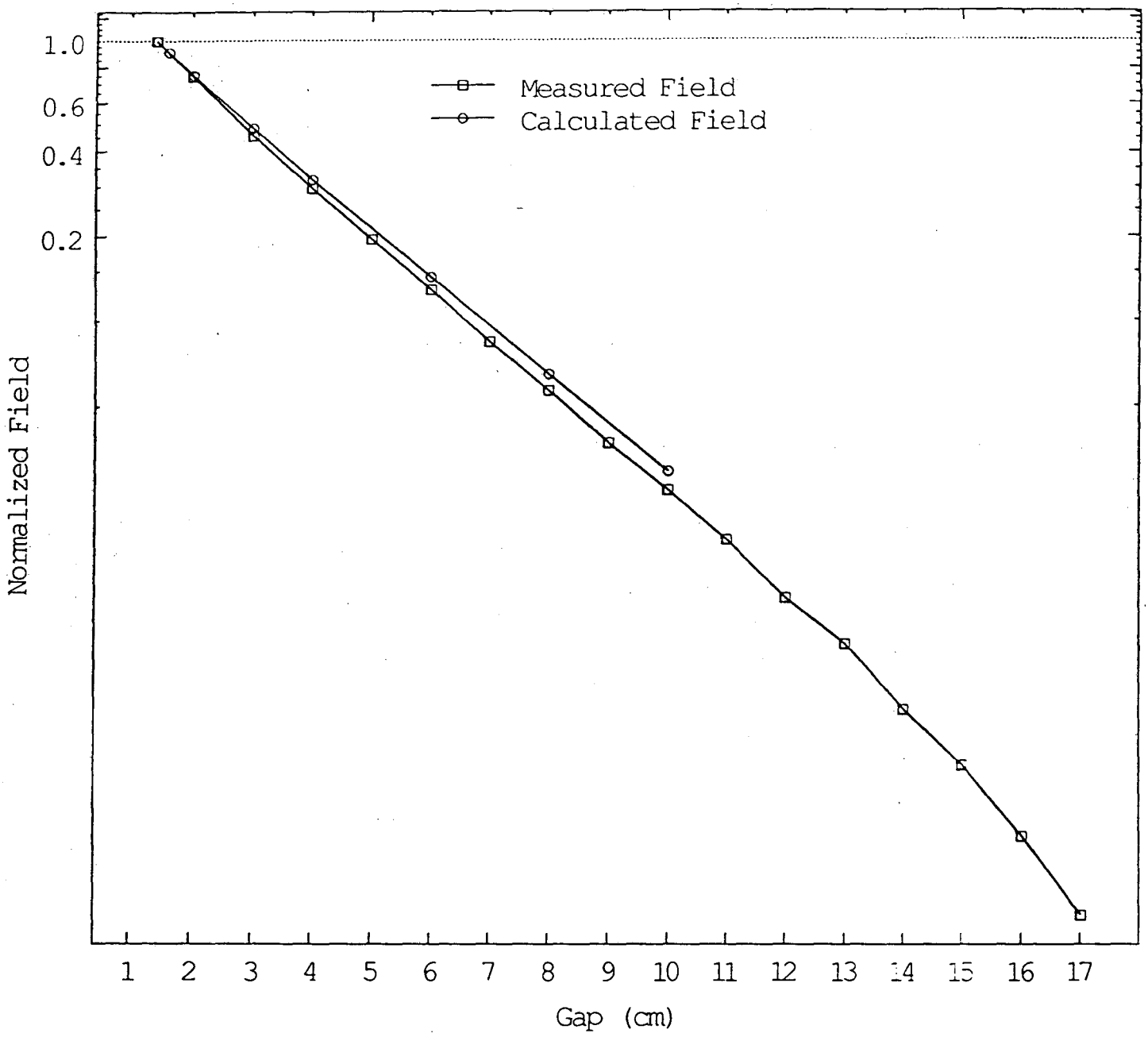
1.0
0.6
0.4
0.2
Normalized Field
Measured Field
Calculated Field
1
2
3
4
5
6
7
8
9
10
11
12
13
14
15
16
17
Gap (cm)

Fig. 7.

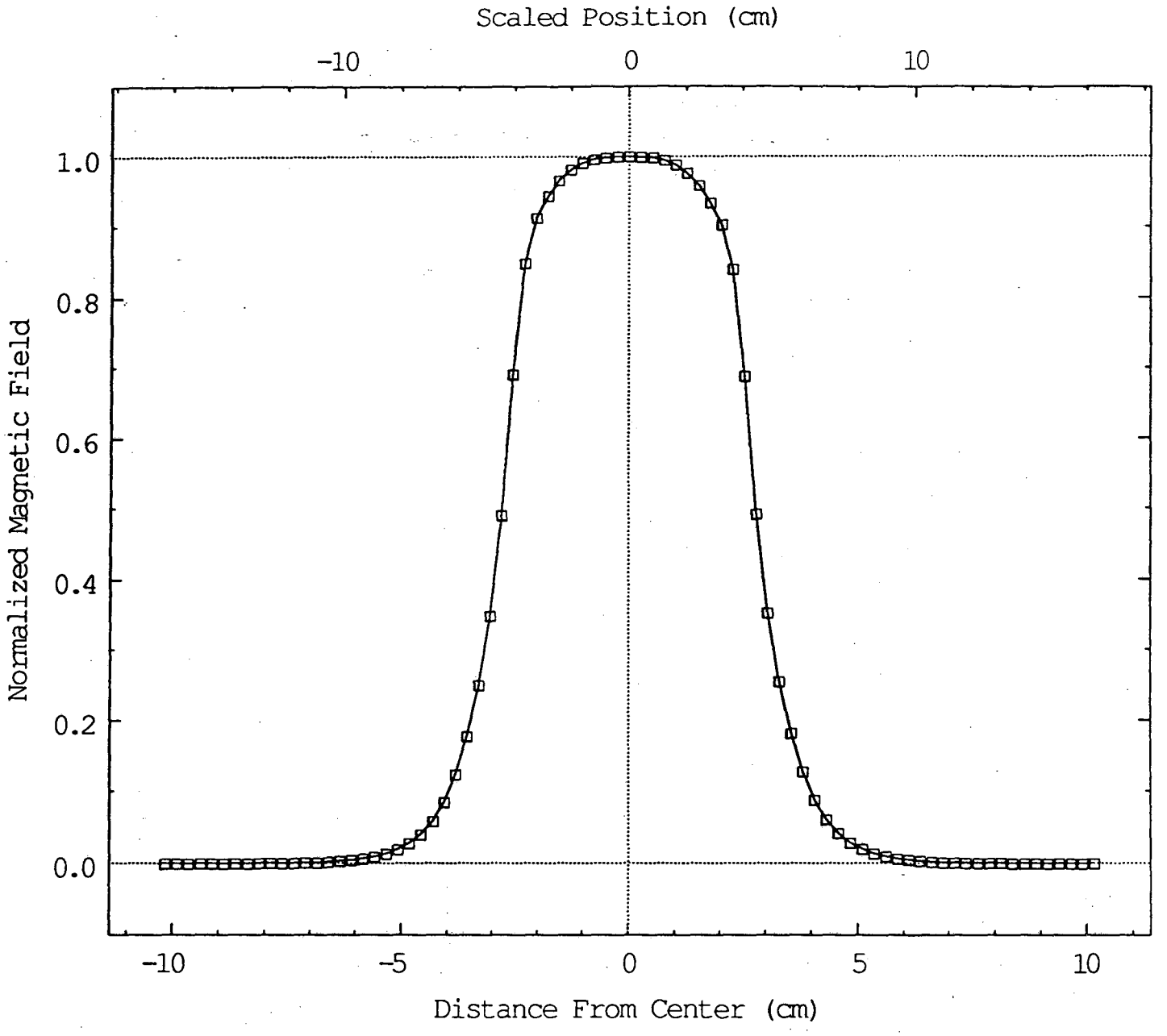
Scaled Position (cm)
-10
0
10
1.0
0.8
0.6
0.4
0.2
0.0
Normalized Magnetic Field
-10
-5
0
5
10
Distance From Center (cm)

Fig. 8.

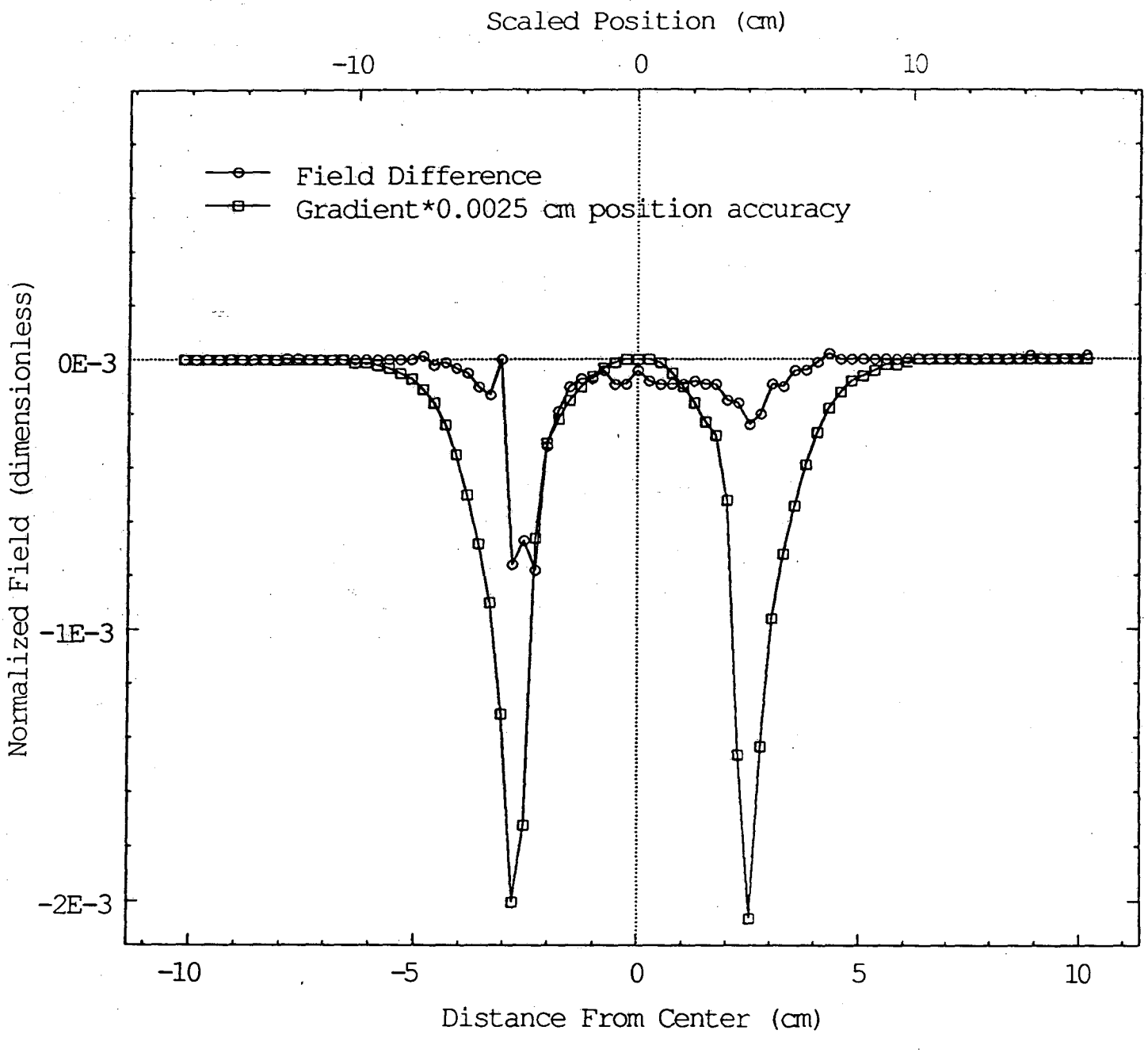
Scaled Position (cm)
-10
0
10
Field Difference
Gradient*0.0025 cm position accuracy
Normalized Field (dimensionless)
0E-3
-1E-3
-2E-3
-10
-5
0
5
10
Distance From Center (cm)

Fig. 9.

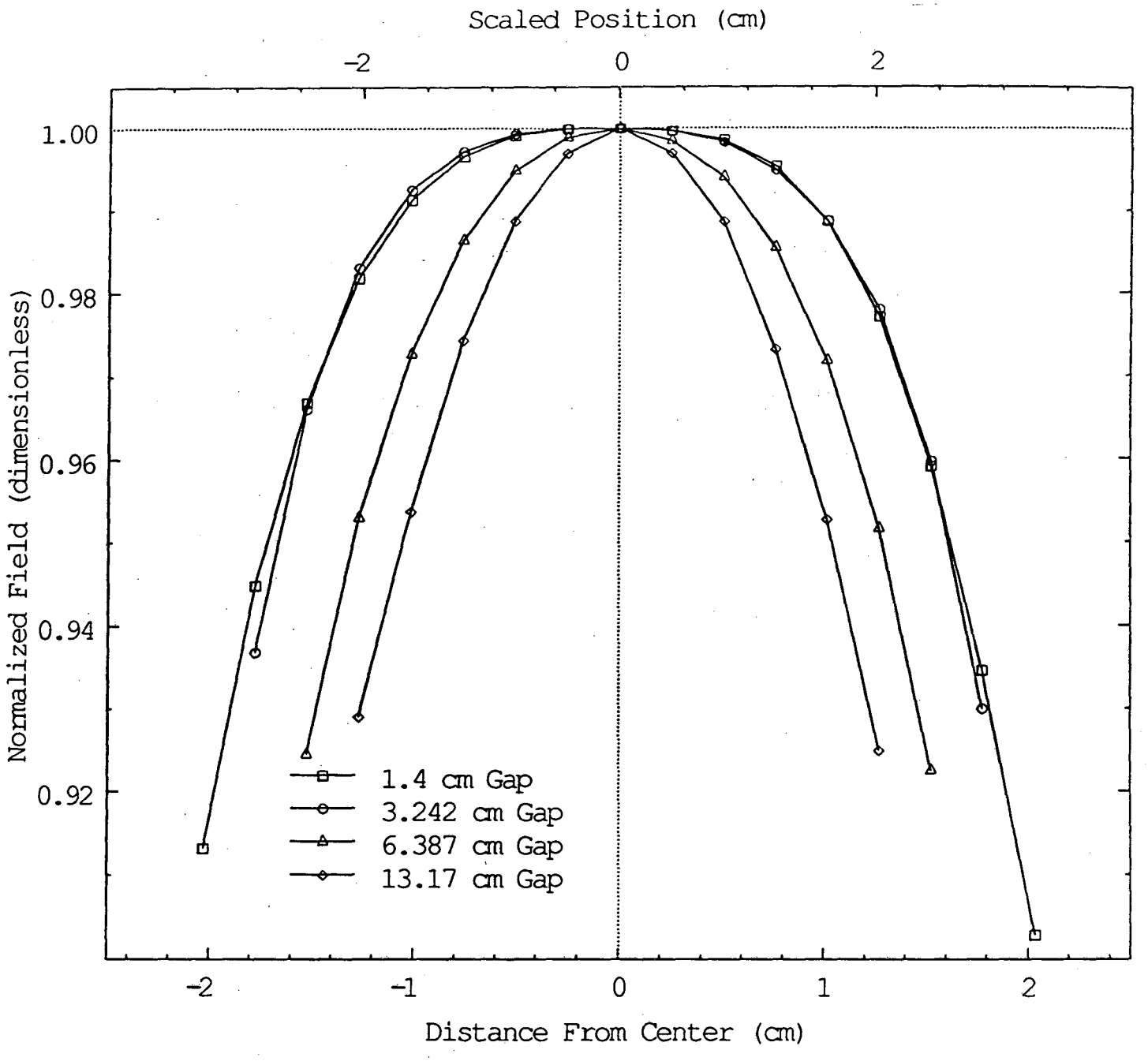
Scaled Position (cm)
-2
0
2
1.00
0.98
0.96
0.94
0.92
Normalized Field (dimensionless)
1.4 cm Gap
3.242 cm Gap
6.387 cm Gap
13.17 cm Gap
-2
-1
0
1
2
Distance From Center (cm)

Fig. 10.

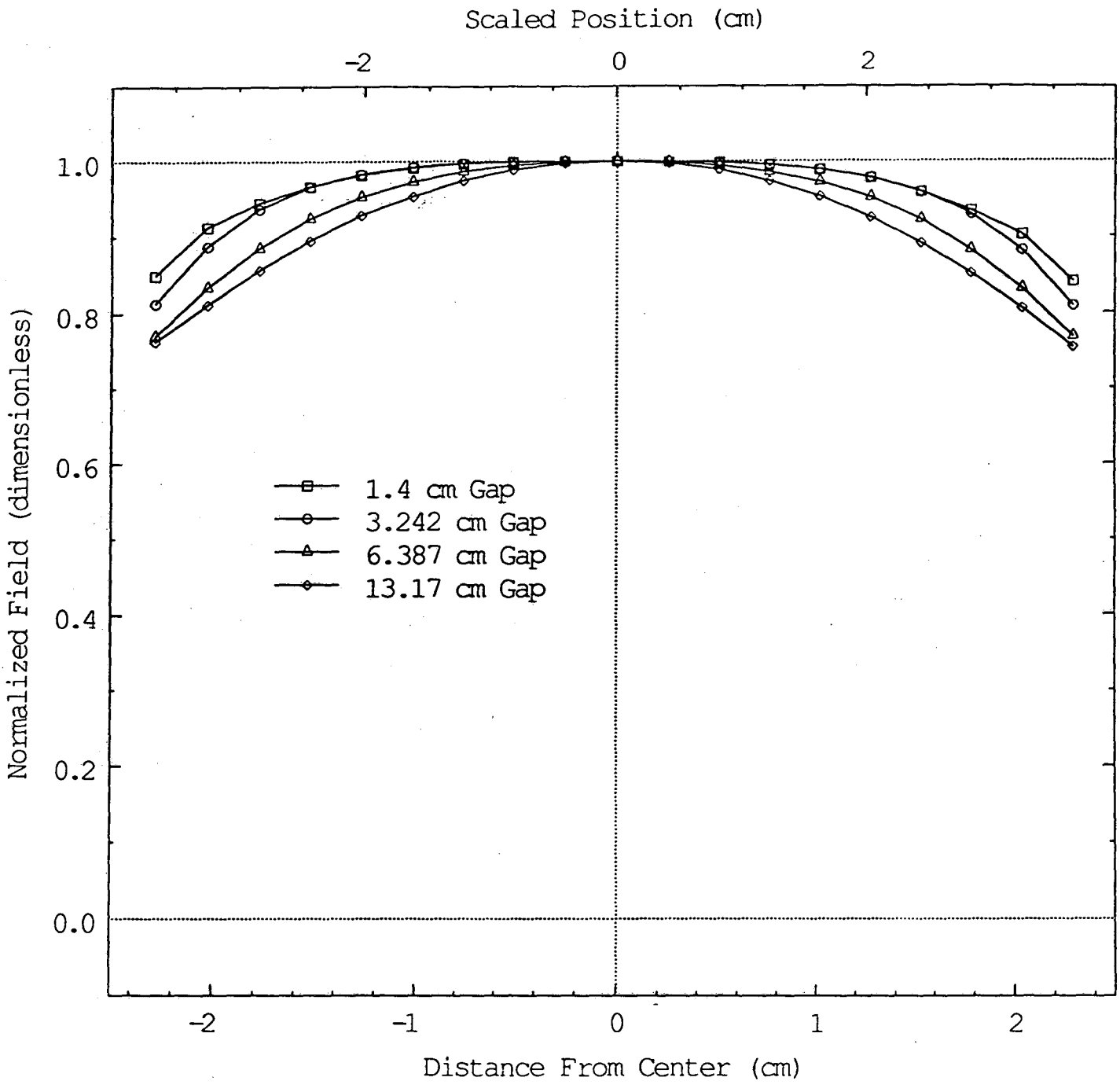
Scaled Position (cm)
-2
0
2
1.0
0.8
0.6
0.4
0.2
0.0
Normalized Field (dimensionless)
1.4 cm Gap
3.242 cm Gap
6.387 cm Gap
13.17 cm Gap
-2
-1
0
1
2
Distance From Center (cm)

Fig. 11.

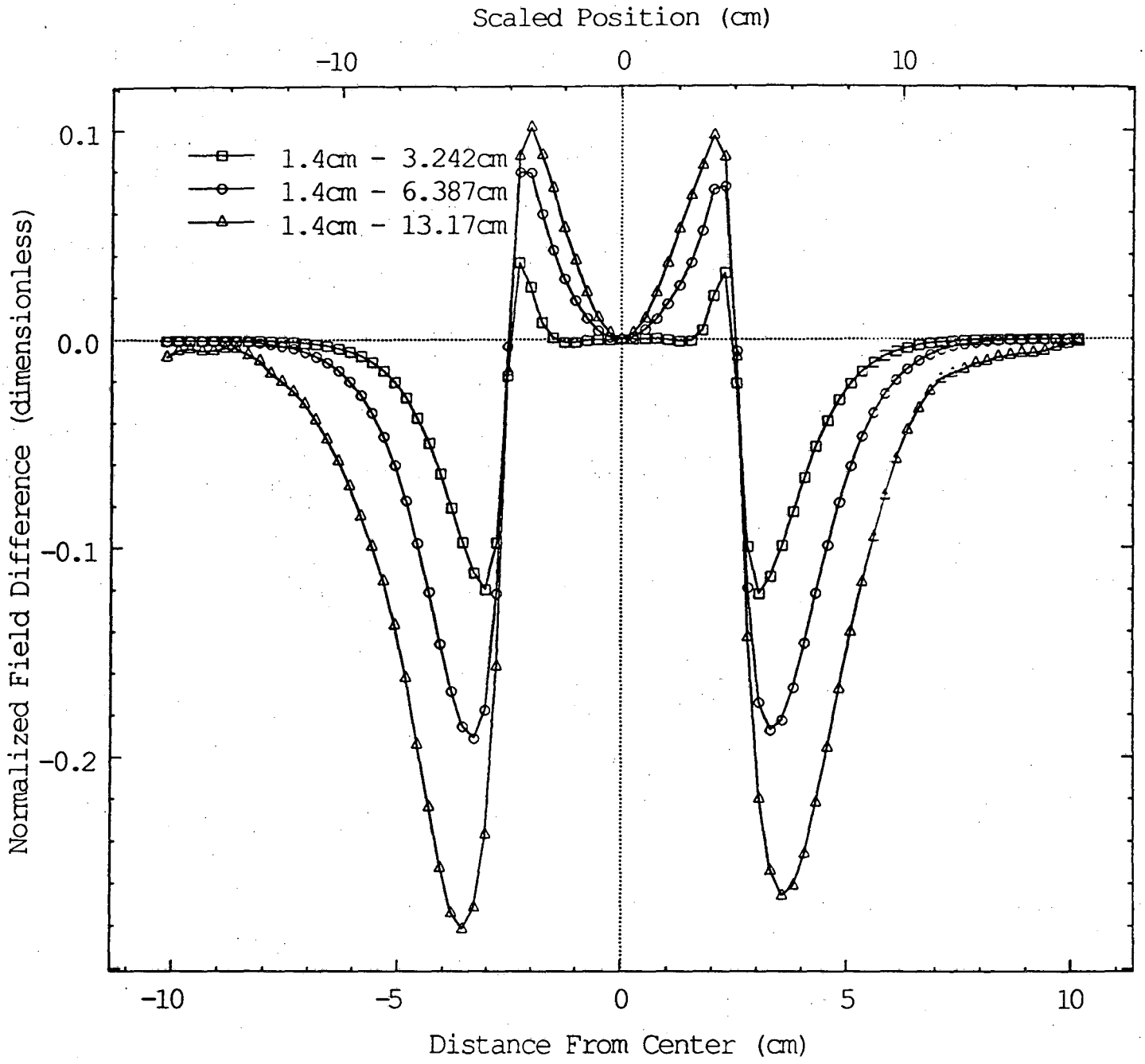
Scaled Position (cm)
-10
0
10
0.1
0.0
-0.1
-0.2
1.4cm - 3.242cm
1.4cm - 6.387cm
1.4cm - 13.17cm
Normalized Field Difference (dimensionless)
-10
-5
0
5
10
Distance From Center (cm)

Fig. 12.

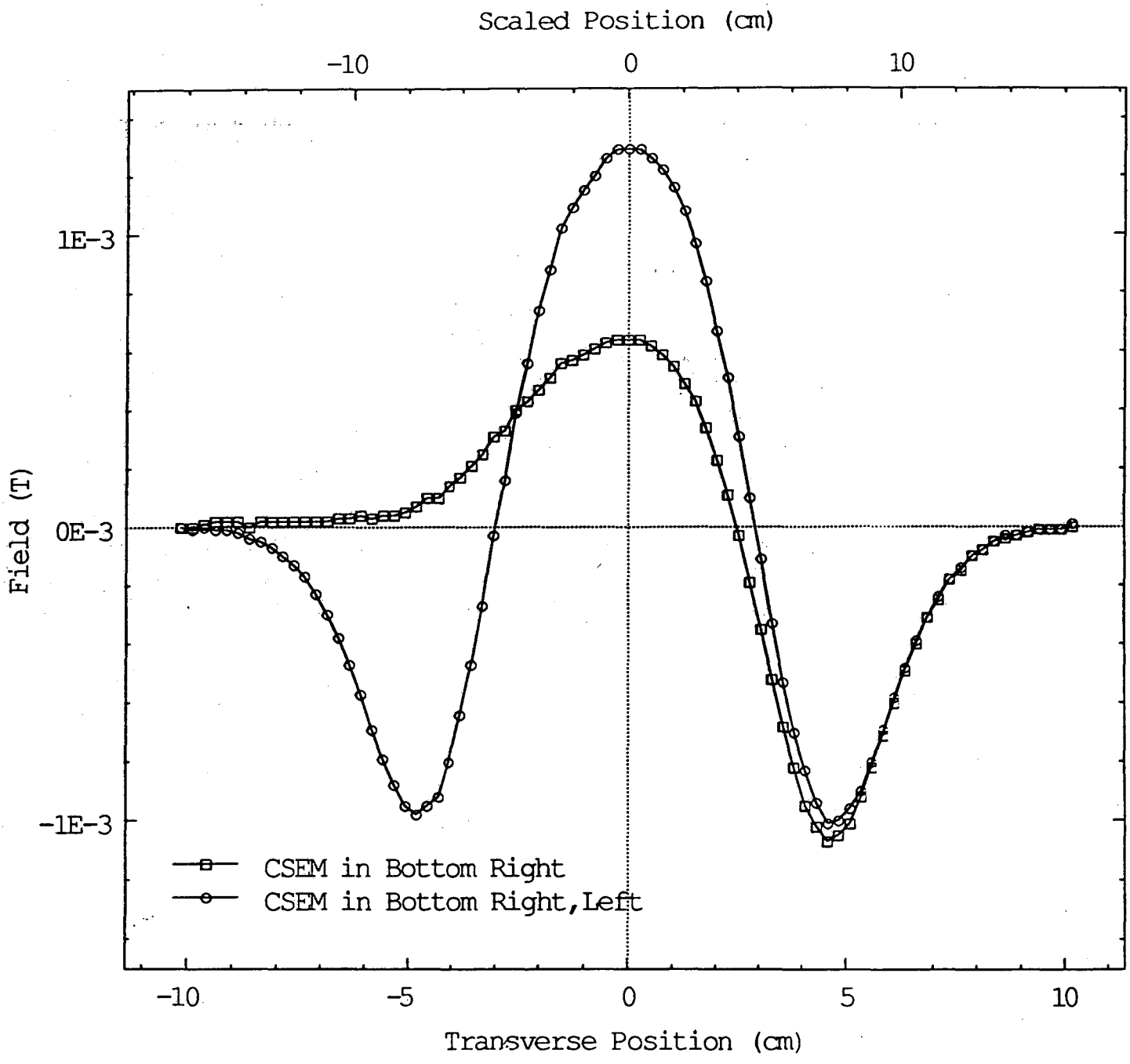
Scaled Position (cm)
-10
0
10
1E-3
0E-3
-1E-3
Field (T)
CSEM in Bottom Right
CSEM in Bottom Right,Left
-10
-5
0
5
10
Transverse Position (cm)

Fig. 13.

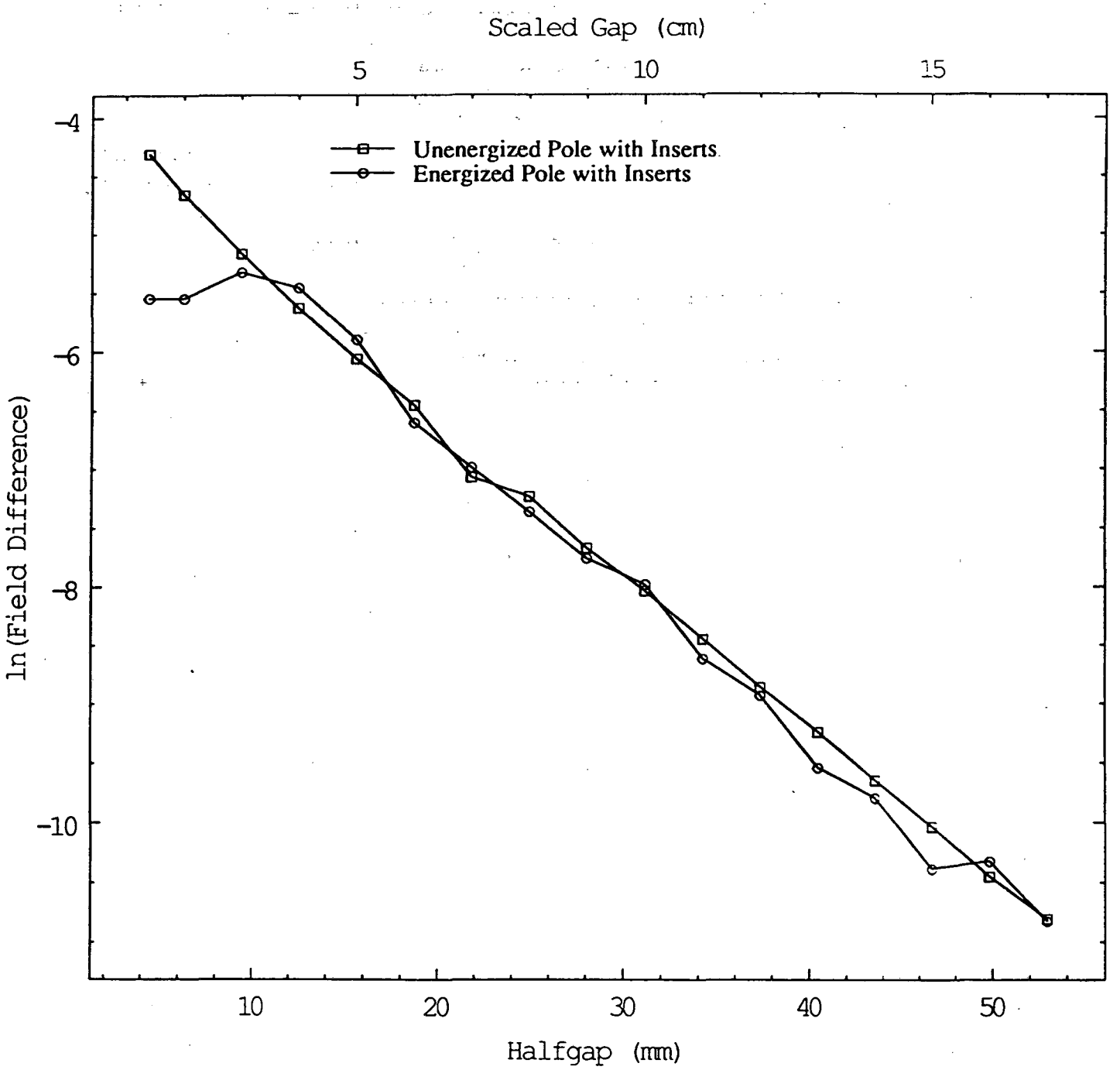
Scaled Gap (cm)
5
10
15
-4
-6
-8
-10
ln(Field Difference)
Unenergized Pole with Inserts
Energized Pole with Inserts
10
20
30
40
50
Halfgap (mm)

Fig. 14.

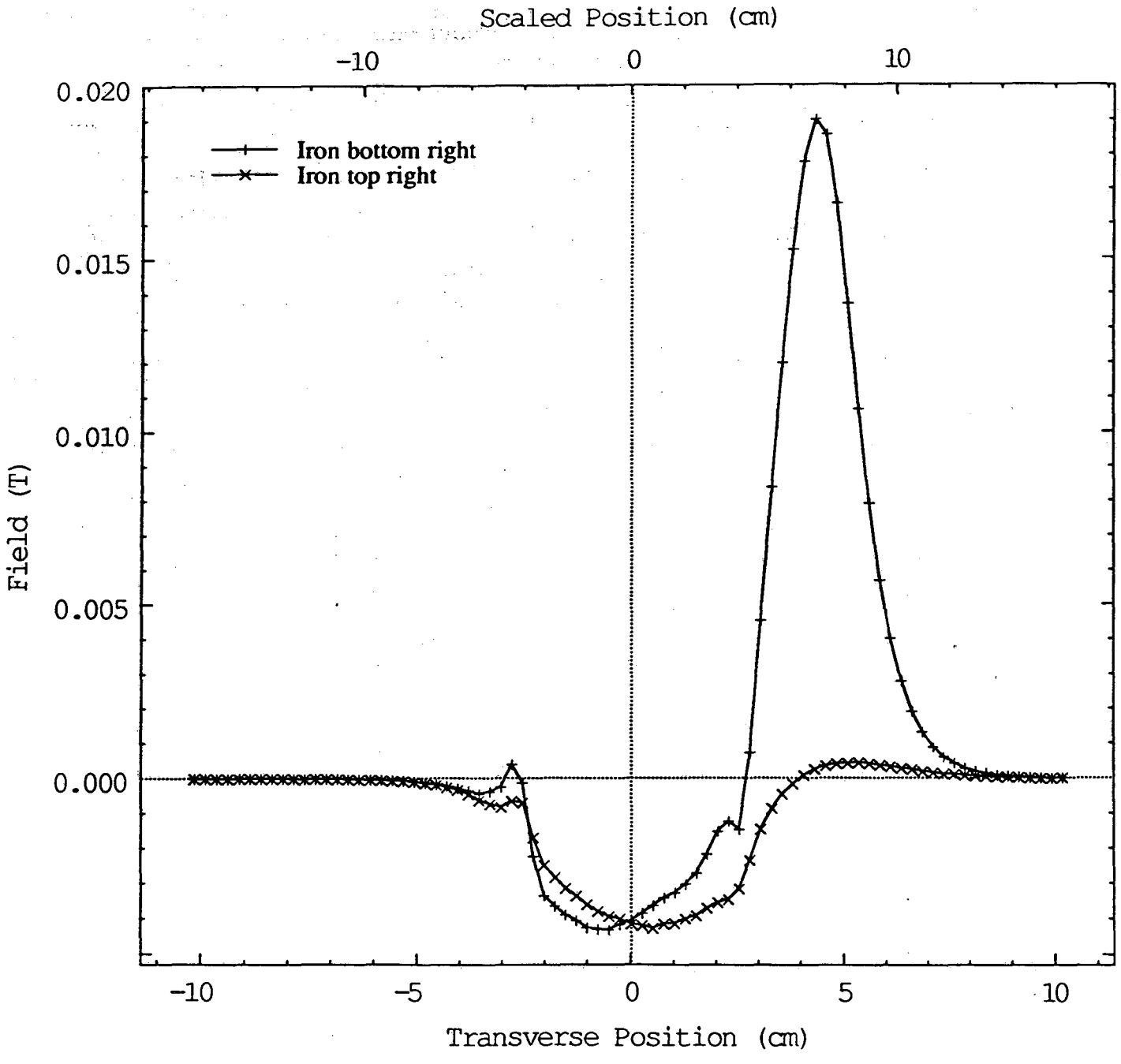
Scaled Position (cm)
-10
0
10
0.020
0.015
0.010
0.005
0.000
Field (T)
Iron bottom right
Iron top right
-10
-5
0
5
10
Transverse Position (cm)

Fig. 15.

LAWRENCE BERKELEY LABORATORY
UNIVERSITY OF CALIFORNIA
TECHNICAL INFORMATION DEPARTMENT
BERKELEY, CALIFORNIA 94720